Electronic Supplementary Material (ESI) for RSC Advances.
This journal is © The Royal Society of Chemistry 2016

Electronic Supplementary Information

Electrochemiluminescence-molecular logic gates based on MCNTs for the multiplexed analysis of mercury (II) and silver (I) ions

Haiyun Liu,[a] Lina Zhang,[b] Meng Li,[a] Mei Yan,[a] Mei Xue,[c] Yan Zhang,[a] Min Su,[a] Jinghua Yu[a] and Shenguang Ge[a]†

[a] Key Laboratory of Chemical Sensing & Analysis in Universities of Shandong, School of Chemistry and Chemical Engineering, University of Jinan, Jinan 250022, P. R. China

[b] Shandong Provincial Key Laboratory of Preparation and Measurement of Building Materials, University of Jinan, Jinan 250022, P. R. China

[c] College of Chemistry, Chemical Engineering and Materials Science, Shandong Normal University, Jinan, 250014, P. R. China

Selectivity of the logic system

To test the selectivity of the sensing system, other metal ions were used in place of Hg^{2+} and Ag^{+}. We systemically challenged the assay with 11 interference metal ions. Fig. S1 depicts the OR system activated with 11 interference metal ions of high concentration (10 μM) and Hg^{2+} (10 nM), Ag^{+} (10 nM). Clearly, the reference metal ions did not interfere with the OR logic system even present with a higher concentration, demonstrating high selectivity of this sensing system for detecting Hg^{2+} and Ag^{+}.

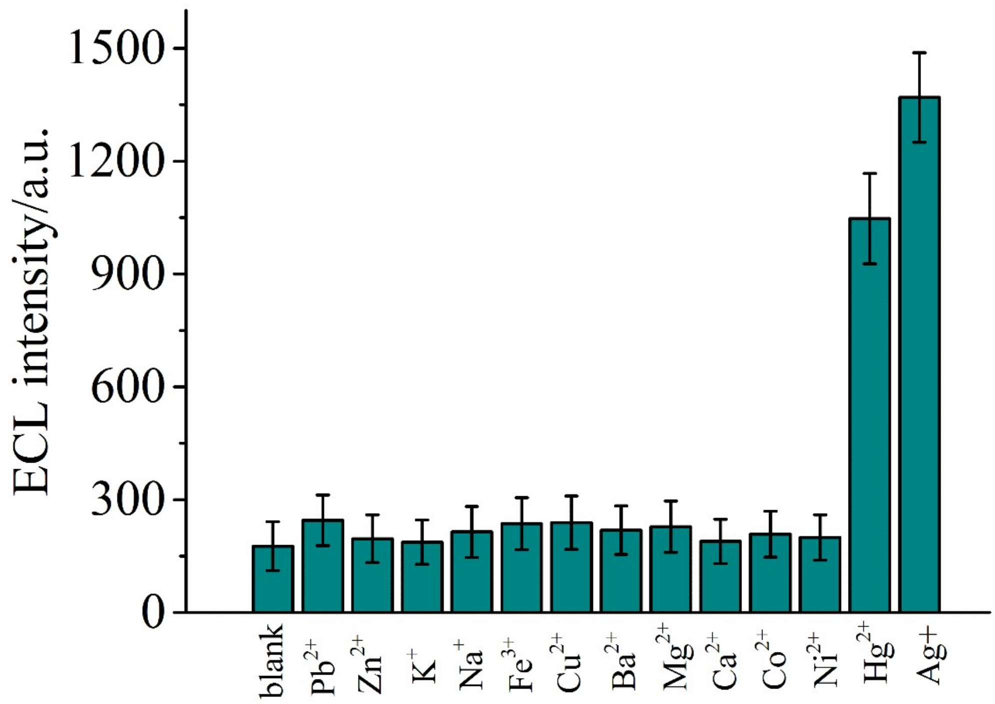

Fig. S1 ECL detection of Hg^{2+}, Ag^{+} ions or other metal ions, such as Pb^{2+}, Zn^{2+}, K^{+}, Na^{+}, Fe^{3+}, Cu^{2+}, Ba^{2+}, Mg^{2+}, Ca^{2+}, Co^{2+}, Ni^{2+} in the OR logic gate. The concentrations for Hg^{2+}, Ag^{+} and other metal ions are of 10 nM, 10 nM and 10 μM, respectively.

INHIBIT gate

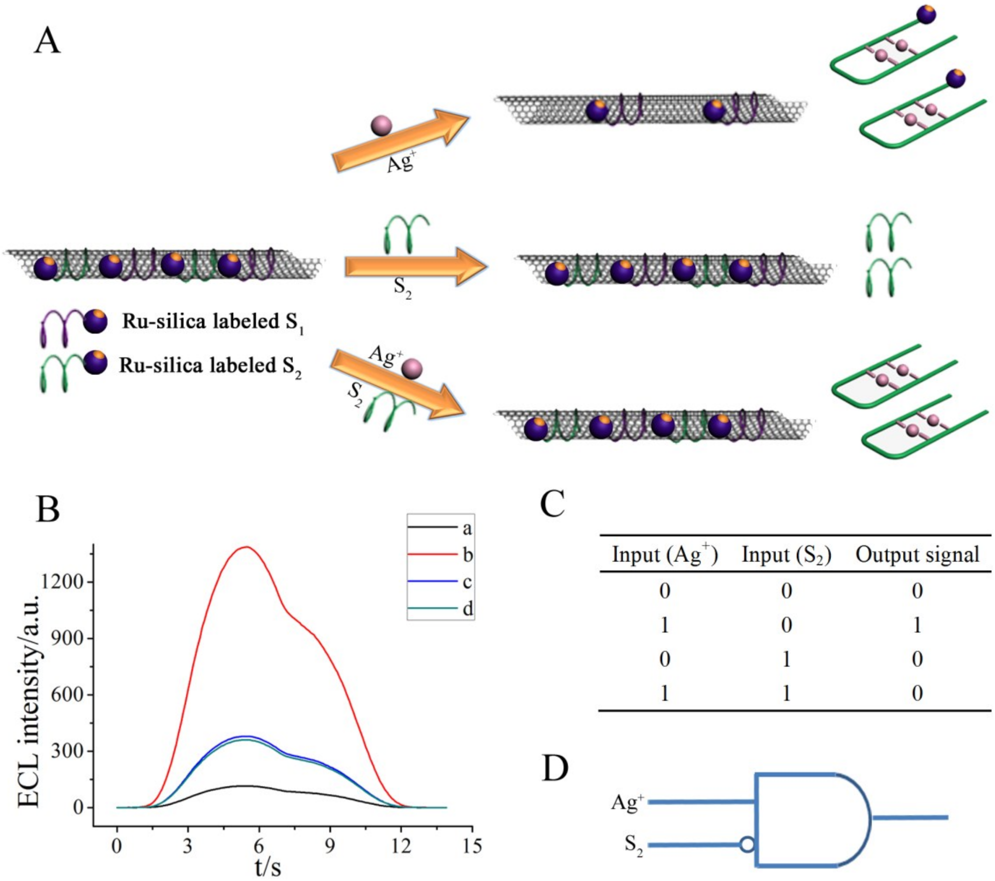

Input (Ag^{+})	Input (S_2)	Output signal
0	0	0
1	0	1
0	1	0
1	1	0

Fig. S2 (A) Schematic representation of the INHIBIT logic gate based on MCNTs/Ru-silica labeled S_1/Ru-silica labeled S_2 complex. (B) ECL intensity vs time curves of the INHIBIT logic gate: (a) MCNTs/Ru-silica labeled S_1/Ru-silica labeled S_2 complex. (b) MCNTs/Ru-silica labeled S_1/Ru-silica labeled S_2 complex treated with 10 nM Ag^{+}. (c) MCNTs/Ru-silica labeled S_1/Ru-silica labeled S_2 complex treated with 2 μM S_2. (d) MCNTs/Ru-silica labeled S_1/Ru-silica labeled S_2 complex treated with 10 nM Ag^{+} and 2 μM S_2. (C) The truth table of the INHIBIT logic gate. (D) The symbol of the INHIBIT logic gate.

We designed another INHIBIT logic gate for Ag^{+} in the similar way as the previous INHIBIT logic gate by using Ag^{+} and S_2 as inputs, which was expressed in

Fig. S2A. Fig. S2B showed the ECL intensity of MCNTs/Ru-silica labeled S_1/Ru-silica labeled S_2 complex at different conditions. The ECL intensity of Ru-silica labeled S_2 was restored upon the addition of Ag^+, which bound with Ru-silica labeled S_2 and induced the recovery of the ECL intensity of Ru-silica nanoparticles. Apparent increase of the ECL intensity was not obtained after the addition of S_2. However, the ECL intensity was decreased largely when the mixture of S_2 and Ag^+ was added, which was because that C-Ag^+-C complex was formed commendably and suppressed the Ag^+-induced ECL recovery of Ru-silica nanoparticles. The results were also in accord with the truth table of the INHIBIT logic gate (Fig. S2C).

NOR gate

We built another NOR logic gate for Ag^+ in the similar way as the previous NOR logic gate by using S_2 and cysteine (Cys) as inputs, which was expressed in Fig. S3A. Fig. S3B showed the ECL intensity of MCNTs/Ru-silica labeled S_1/Ru-silica labeled S_2 complex at different conditions. When there was no input, the ECL intensity of Ru-silica labeled S_2 was restored, which was because that Ag^+ bound with Ru-silica labeled S_2 and induced the recovery of the ECL intensity of Ru-silica nanoparticles. In the logic gate, unlabeled S_2 and Cys could both bind with Ag^+ via forming special structures. Consequently, inputting any one or both of them, the Ag^+-induced recovery of the ECL intensity of the Ru-silica could be inhibited, indicating that both S_2 and Cys prevented the desorption of Ru-silica labeled S_2 from MCNTs. The truth table of the resulting NOR logic gate was given in the Fig. S3C.

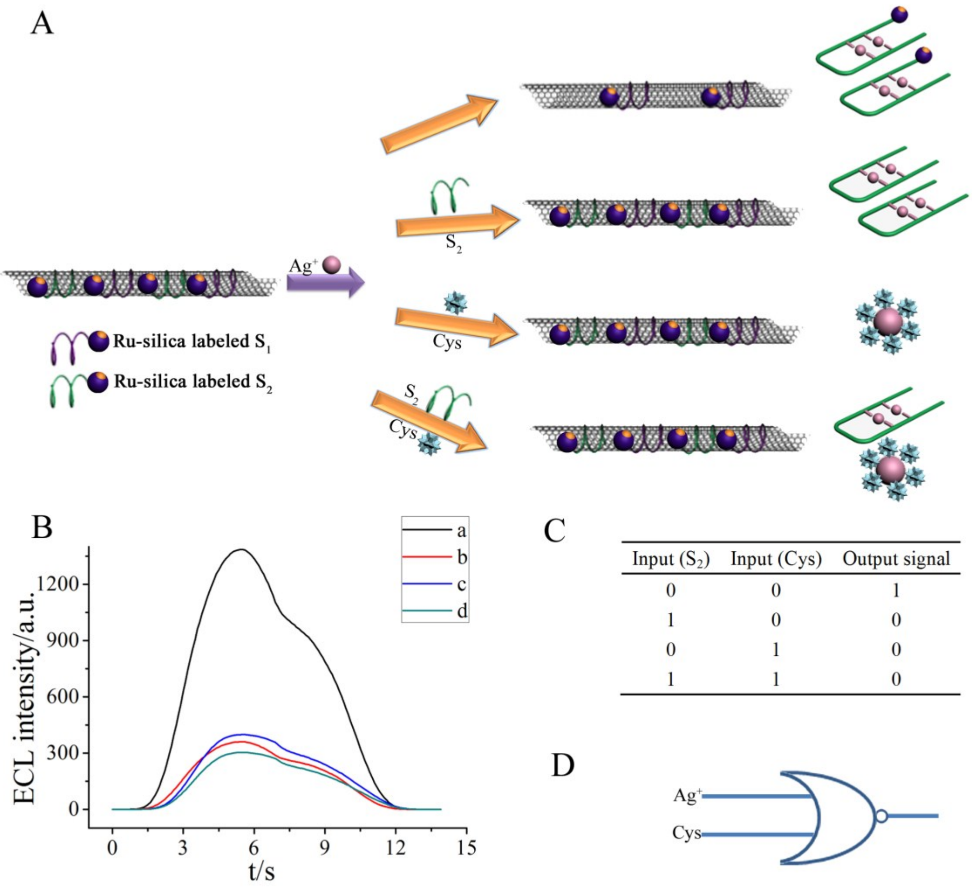

Fig. S3 (A) Schematic representation of the NOR logic gate based on treated MCNTs/Ru-silica labeled S_1/Ru-silica labeled S_2 complex by 10 nM Ag^+. (B) ECL intensity vs time curves of the NOR logic gate: (a) The treated MCNTs/Ru-silica labeled S_1/Ru-silica labeled S_2 complex by 10 nM Ag^+. (b) The treated MCNTs/Ru-silica labeled S_1/Ru-silica labeled S_2 complex by 10 nM Ag^+ was then treated with 2 μM S_2. (c) The treated MCNTs/Ru-silica labeled S_1/Ru-silica labeled S_2 complex by 10 nM Ag^+ was then treated with 300 nM Cys. (d) the treated MCNTs/Ru-silica labeled S_1/Ru-silica labeled S_2 complex by 10 nM Ag^+ was then treated with 2 μM S_2 and 300 nM Cys. (C) The truth table of the NOR logic gate. (D) The symbol of the NOR logic gate.

Analytical performance of I^- and Cys

Fig. S4A illustrated the ECL intensity changes of the MCNTs/Ru-silica labeled S_1/Ru-silica labeled S_2 complex upon addition of various concentrations of I^- when the concentration of Hg^{2+} was 10 nM. A linear relationship between the ECL intensity and the concentrations of I^- over a range of 100 nM to 10μM (inset of Fig. S4A) was obtained by analyzing the change of ECL intensity with the concentrations of I^-. In addition, Fig. S4B was the ECL intensity changes of the MCNTs/Ru-silica labeled S_1/Ru-silica labeled S_2 complex upon addition of various concentrations of Cys when the concentration of Ag^+ was 3 nM. As shown in the inset of Fig. S4B, the ECL intensity was linear over the logarithm of Cys concentration ranging from 3 to 300 nM. The detection limits of I^- and Cys were 0.1μM and 10 nM, respectively.

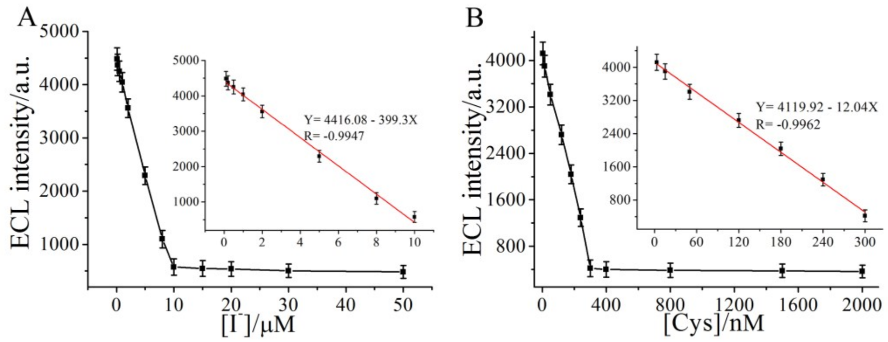

Fig. S4 Relationship between ECL intensity and (A) I^- and (B) Cys concentration in pH 7.4 PBS containing 1.0×10^{-5} mol·L^{-1} TPA. Inset: Calibration curve of the ECL signals for (A) I^- and (B) Cys, respectively.